

Studies on Biaxial Stretching of Polypropylene Film. X. High-Temperature X-Ray and Optical Study of Type III Orientation

NOBORU IWATO, HIROSHI TANAKA, and SABURO OKAJIMA,*
*Faculty of Technology, Tokyo Metropolitan University,
Setagaya-ku, Tokyo, Japan*

Synopsis

Change of orientation and crystalline state of uniaxially stretched polypropylene film during subsequent restretching with the film width unrestrained was studied by means of x-ray, optical, and calorimetric methods. Uniaxially stretched film immediately after 5 min of preheating at 130°C barely suffers premelting. When the preheating temperature rises above 150°C, the premelting proceeds gradually and the x-ray pattern becomes a halo around 160°C, which, however, returns nearly to the original crystalline pattern after cooling to room temperature. The fraction premelted in the preheating amounts to about $1/2$ - $2/3$ under the condition yielding type III orientation at room temperature, as previously reported. The 130°C restretching brings type II orientation already at that temperature, similar to what has been observed at room temperature. When the restretching is performed above 155°C, the crystalline pattern remaining after the preheating converts to a halo during the restretching, which, however, converts again to the crystalline pattern of type III orientation when it is rapidly cooled. This suggests that the restretching at higher temperatures breaks up lamellae into smaller-sized crystallites. Upon cooling, the smaller-sized crystallites reorganize lamellae, the deformed lattice recovers its ordinary state, and the pulled-out chains crystallize into intermolecular crystallites, aligning in the direction of restretching. Concurrently, disorientation proceeds fairly rapidly at such high temperatures, hence, type III orientation cannot be observed even at room temperature unless the film is quickly cooled after restretching. It is concluded that type III orientation results from restretching when thermal motion of the chains within the crystalline phase becomes so violent that the unfolding occurs easily as compared with lamellar rotation.

INTRODUCTION

In the preceding paper,¹ the author reported that when a uniaxially stretched polypropylene film is progressively stretched in the direction perpendicular to that of the first stretching, *pp*,² with the film width unrestrained (the second step of biaxial stretching in two steps), the orientation axis splits in two. These rotate gradually in the opposite directions toward the restretching axis, *ps*² (type II orientation). However, when

* Present address: Faculty of Engineering, Yamagata University, Yonezawa, Yamagata-ken, Japan.

the restretching temperature, T_2 , is about 20°C higher than the stretching temperature, T_1 , another type of orientation (type III orientation) develops. This new type of orientation appears also when the film width is restrained during the restretching, even though T_2 is equal to T_1 . The x-ray photographs (*thru*) of the samples possessing this latter type of orientation always show the existence of two orientation axes lying parallel to pp and ps , respectively, and the x-ray diffraction intensities ($hk0$) on the meridian (parallel to pp) increase at the expense of those on the equator (parallel to ps) as the restretching proceeds.

The authors suggested that there are different mechanisms of orientation for these two types of deformation; in type II, the rotation of lamellar crystal stack resulting from the first stretching plays a principal role, while in type III, unfolding of molecules from lamellar crystals and recrystallization into intermolecular crystals aligning parallel to ps may be predominant. Relative easiness of the rotation of lamellar crystals as compared with the unfolding of molecules from the lamellar crystals should determine the type of orientation. Even when the film width is unrestrained during the restretching, sufficiently higher T_2 (more than 20°C above T_1) enhances the unfolding because of the violent thermal motion of molecular chains within the crystalline phase and brings about type III orientation. In this paper, the authors present some experimental support for this view concerning the mechanisms of restretching.

EXPERIMENTAL

A piece of 850- μ -thick film (B_3^3 , tacticity 96%, \bar{M}_n 29×10^4) was melt pressed at 210°C, followed by quenching in ice water. This piece was uniaxially stretched 4 \times at a velocity of 100%/min at 130°C in a polyethylene glycol bath, which was used as the sample for subsequent stretching in air.

Restretching at T_2 was carried out in a small bronze cell with an aluminum foil window, with which an x-ray diffractometer (Rota-flex RU-3V

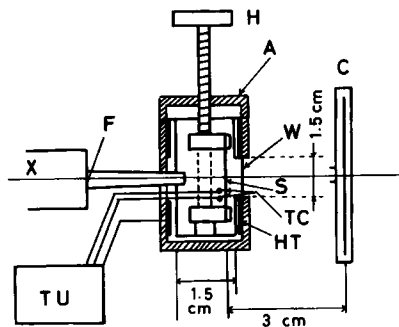


Fig. 1. Stretching cell assembled into x-ray diffractometer: (X) x-ray beam; (F) nickel foil filter; (A) insulator (asbestos); (W) aluminum foil window; (S) sample; (TC) thermocouples; (HT) heater; (H) hand screw; (C) photograph film; (TU) temperature control unit.

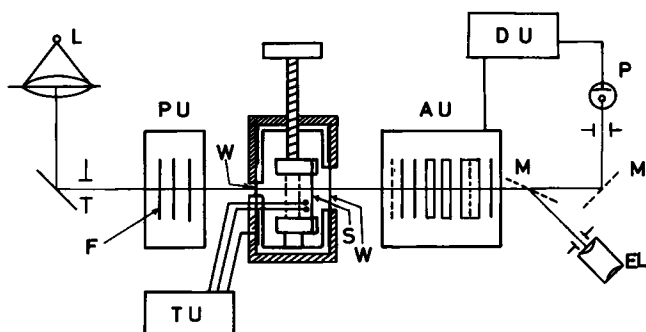


Fig. 2. Stretching cell assembled into ellipsometer: (L) light source; (PU) polarizer unit; (F) interference filter; (W) glass window; (TU) temperature control unit; (S) sample; (AU) analyzer unit; (M) mirror; (P) photoelectric cell; (DU) display unit; (E) eye piece lens.

of Rigaku Denki Co., Ltd.) was equipped, as shown in Figure 1. A piece of the sample, $1.5\text{--}2 \times 1.7$ cm, was mounted on a small stretcher, which was placed in the cell and stretched by a hand screw. The stretching was finished in 1–2 min. The cell was heated electrically and the temperature of the sample was measured and controlled by means of two thermocouples placed in contact with the sample film. Two min of exposure ($\text{Cu K}\alpha$ radiation, 45 kV and 100 mA) was used for x-ray photographic strokes. In a few cases, however, 15 sec of exposure was used. For this reduction of the exposure time, a fluorescent screen was placed in contact with the back of the photographic film and the thinner aluminum foil was used.

For the optical study, a similar cell with two glass windows was assembled into an ellipsometer constructed by Nippon Kogaku K.K. (Fig. 2). Ten sec to 2 min was necessary for an automatic computation of retardation by this apparatus.

Thermal analysis was performed by using a Perkin Elmer differential scanning calorimeter (DSC 1B) which was run at a heating rate of $16^\circ\text{C}/\text{min}$.

RESULTS

X-Ray Observation

In order to study the change by thermal treatment in the diffraction patterns before restretching, the sample specimen was placed in the cell, which was heated up to T_2 ($130\text{--}160^\circ\text{C}$) from room temperature in 15 min, and x-ray photographs were obtained without restretching. The diffraction patterns from aluminum and polypropylene appear to overlap on a photograph; however, they are easily discriminated from each other.

In Figure 3, $a_1\text{--}d_1$ are the photographs taken at T_2 , while $a_2\text{--}d_2$ are those taken after subsequent cooling to room temperature. Photograph a_1 is

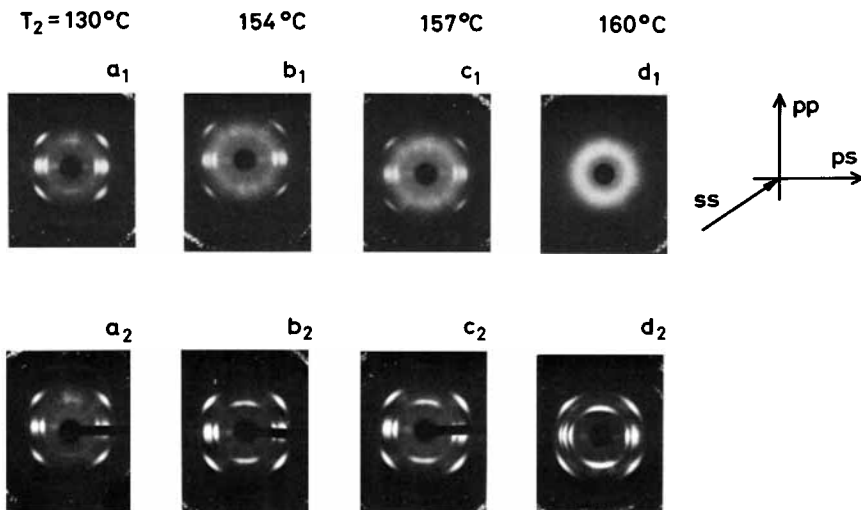


Fig. 3. X-Ray photograph of uniaxially stretched film taken at T_2 (a_1 - d_1) and film taken after cooling to room temperature (a_2 - d_2).

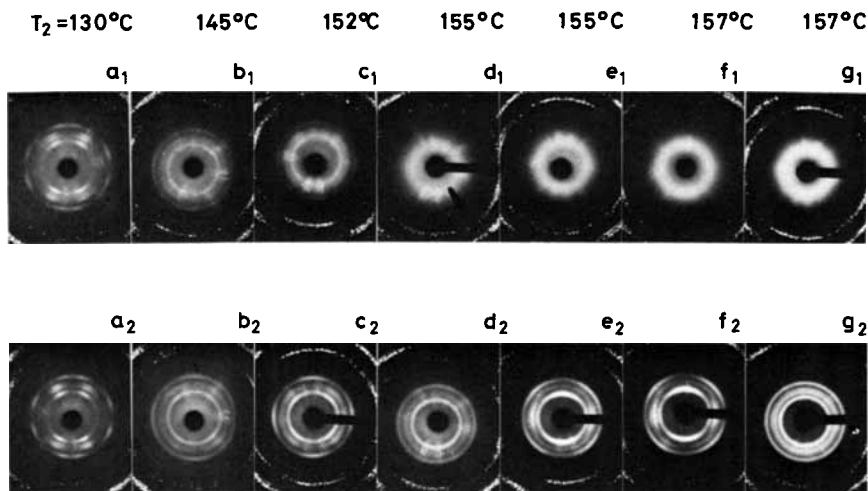


Fig. 4. X-Ray photographs taken immediately after the restretching (a_1 - g_1) and after subsequent cooling to room temperature (a_2 - g_2). Restretching¹: $[2-2FI](130-T_2)_{p-\sigma}$ (4×2.5 or 3). (The film stretched uniaxially $4 \times$ at 130°C in a polyethylene glycol bath was restretched 2.5 or $3 \times$ in the direction, ps , at T_2 in air.)

still crystalline similar to those at room temperature, while b_1 - d_1 are progressively disordered, and d_1 , heated at 160°C , becomes a halo. Upon cooling to room temperature after such short-time heating, the original order and orientation are nearly completely recovered excepting for the appearance of (110) diffraction on the meridian in b_1 - d_1 , which may be

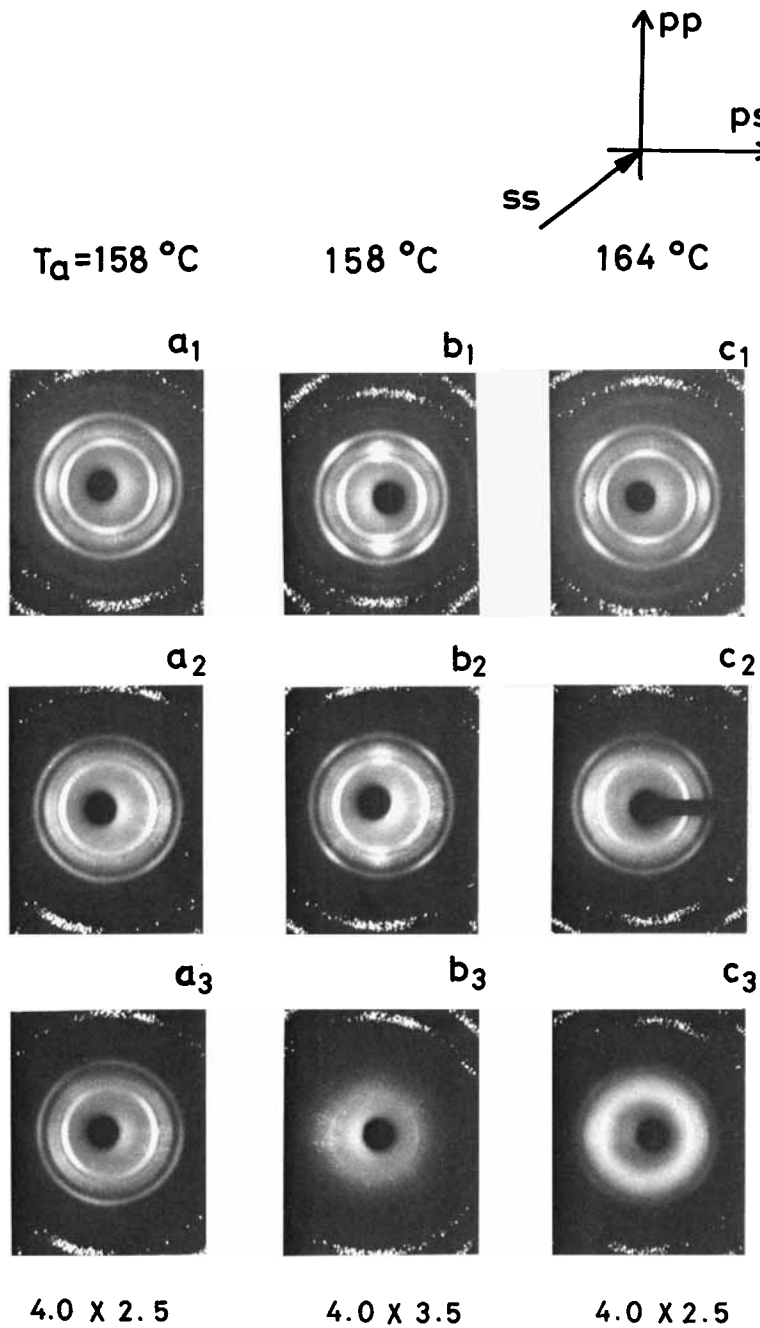


Fig. 5. Change in type III pattern during heating at temperature T_a , slightly higher than T_2 . Film: $[2\text{-}2\text{FI}](130\text{-}157)_p(4.0 \times 2.5 \text{ or } 3.5)$. ($a_1\text{-}c_1$) Pattern at room temperature; ($a_2\text{-}c_2$) pattern after keeping at T_a for 5 min; ($a_3\text{-}c_3$) pattern after keeping at T_a for 15 min.

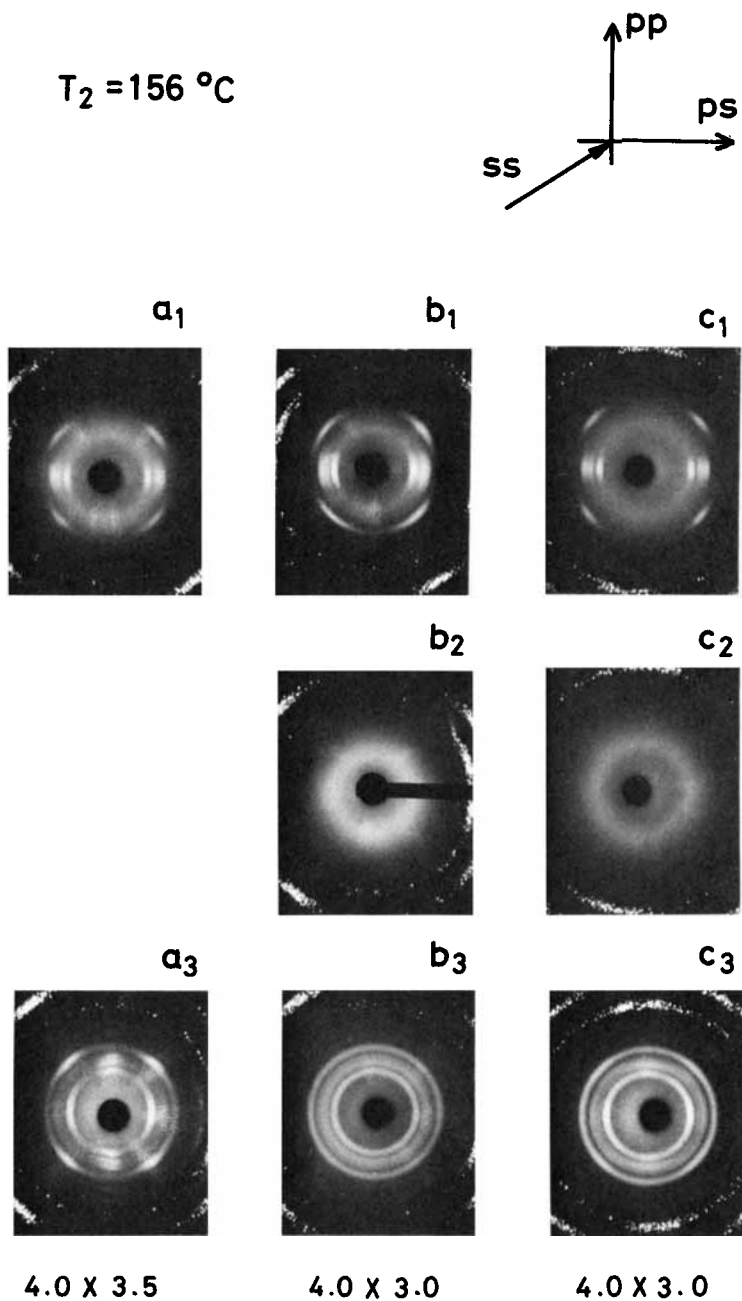


Fig. 6. Change in x-ray pattern during restretching and cooling. (a_1 - c_1) Taken at 156°C immediately before restretching; (b_2) taken at 156°C immediately after restretching; (c_2) taken at 156°C during restretching; (a_3 - c_3) taken after cooling to room temperature; stretching: $[2\text{-2FI}](130\text{-}156)_{p-a}(4 \times V_2)$; exposure: 15 sec for c_2 and 2 min for a_2 and b_2 .

assigned to a^* -axis orientation.⁴ Therefore, partial melting and recrystallization to considerable extent is believed to occur during heating above 154°C. These changes correspond well with the melting behavior as shown later by DSC study.

When restretching was carried out 1–2 min after reaching a specimen temperature of T_2 , followed by x-ray strokes, the photographs shown in Figure 4, a_1 – g_1 were obtained. Those in Figure 4, a_2 – g_2 , are the result of subsequent exposures at room temperature. The restretched film at 130°C clearly exhibits type II orientation at that temperature (a_1). This is not much changed after cooling (a_2); however the patterns of the samples stretched at 145°C and 152°C are still crystalline but so disoriented (b_1 – c_1) that their type II orientation is barely discernible. When T_2 is higher than 155°C, all the patterns are halos (d_1 – g_1).

In comparison with Figure 3, b_1 – d_1 , Figure 4, b_1 – g_1 photographs are considerably disordered, probably because of breaking apart of the crystallites into smaller sizes and lattice distortion due to the restretching force. It is noticeable, however, that the halo changes again to a crystalline pattern at room temperature (d_2 – g_2). Photographs b_2 and c_2 show type II orientation; however, d_2 – g_2 do not indicate type III orientation; irrespectively of their sufficiently higher T_2 , they are rather similar to Figure 3, d_2 . This is believed to indicate that the newly developed crystallites in the ps direction have lower stability in comparison with those aligning in pp . This is more clearly seen in Figure 5, where a film with type III orientation is heated at temperature T_a , slightly higher than its T_2 . The diffraction on the meridian disappears after 5 min in a_2 and c_2 and after 15 min in b_3 , while the diffractions on the equator still remain there in all cases. Such an anisotropic distribution of crystallite stability is important in considering the properties of this type of film.²

In Figure 6, the specimen to be stretched was placed in the cell which had been heated at T_2 , and restretching was begun after 5 min (the temperature of the specimen reached T_2 after 10 min) and photograph was taken at T_2 before (a_1 – c_1) and after (b_2) and during (c_2) the stretching, and again at room temperature (a_3 – c_3) after the restretching. In the case of c_2 , the exposure time was only 15 sec. This shortening of the exposure time was attained by improving the diffractometer as mentioned in the experimental section. However, as shown by Fig. 4, d_1 – g_1 , the diffraction pattern is still a halo; hence, the disordering at this stage is attributable mainly to restretching rather than heating. Of course, this disorientation proceeds concurrently at a considerably higher rate, because the disorientation at room temperature becomes larger with increase in the exposure time at T_2 after the restretching, i.e., in the order $a_3 \rightarrow c_3 \rightarrow b_3$. Photograph a_3 is the diffraction pattern of the sample cooled to room temperature immediately after the restretching without photographing.

From these results, it is concluded that type III orientation is obtained when the specimen is cooled to room temperature immediately after the restretching (a_3 , c_3).

Optical Observation

The change in the retardation,

$$\Gamma = (n_{pp} - n_{ps}) \times d$$

of the uniaxially stretched film while at T_2 was observed, where n_{pp} and n_{ps} are the refractive indices parallel to pp and ps , respectively, and d is the specimen thickness. Figure 7 shows the change in Γ when T_2 is changed from 130°C to 162°C. The temporary cooling of the cell caused by placing the specimen in the cell which was heated at T_2 recovered in 5 min and the lapse after this recovery is taken along the abscissa. It is seen that the higher T_2 , the more rapidly Γ drops especially within the first 5 min. The curve at 130°C or 150°C passes through a minimum value, probably because of premelting and recrystallization. It is difficult to keep the specimen for longer times above 160°C because T_2 is close to the melting point and only one observation could be made.

Upon cooling the specimen, Γ increases as shown by some representative points. The amount of recovery in Γ is a function of the heating temperature and passes through a maximum around $T_2 = 156^\circ\text{C}$. The density of the specimen heated at 130°C for 25 min increases on cooling to 0.9075 g/cm³ from the original value of 0.9055 g/cm³. The comparatively larger increase in Γ above the original value cannot be explained simply by packing effect; rather, it may be attributable to recrystallization and orientation of the partially melted chains on surviving crystals and nuclei which have higher stability and higher orientation than the premelted portion. As T_2 increases, the amount of premelted polymer increases; hence, these recrystallization and orientation effects become larger, resulting in the larger recovery. As T_2 rises further, disorientation and dissociation of the survived crystals and nuclei into single molecules, become conspicuous in line with the increase of the premelted amount; therefore, the recovery in Γ decreases again, yielding a small maximum around 156°C.

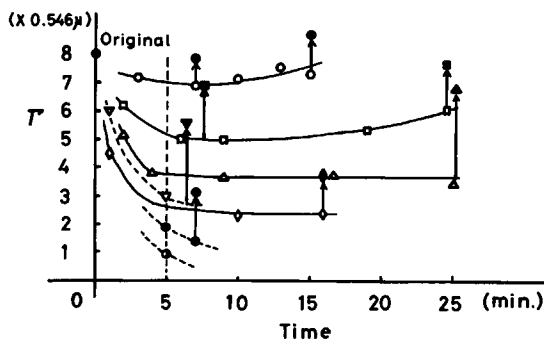


Fig. 7. Change in retardation of uniaxially stretched ($4\times$) film while heating at various temperatures: (○) 130°C; (□) 150°C; (Δ) 154°C; (▽) 156°C; (◇) 158°C; (⊙) 160°C; (●) 162°C. Solid marks (●) indicate values after cooling to room temperature. Wavelength of used light beam is 0.546 μ .

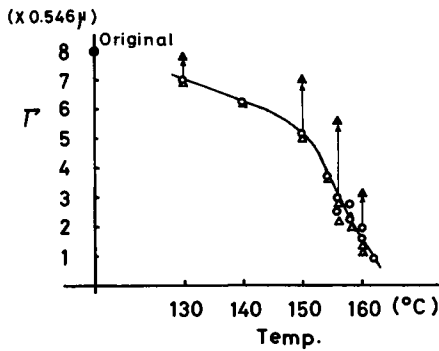


Fig. 8. Relation between retardation of uniaxially stretched film ($4\times$) and temperature: (O) after 5 min; (Δ) after 7 min.

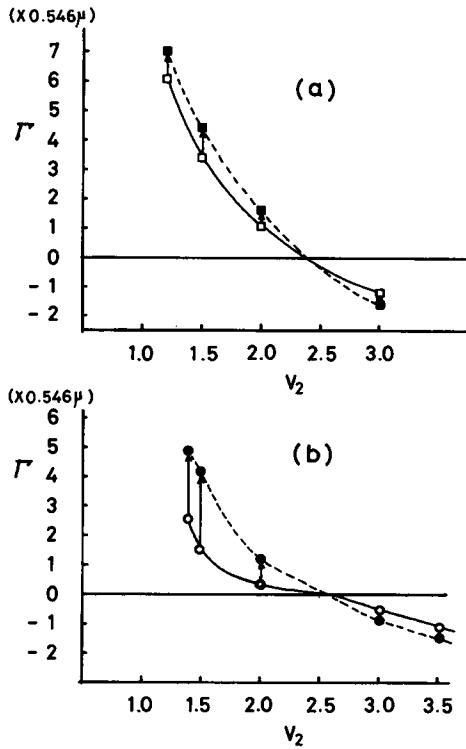


Fig. 9. Retardation of biaxially stretched film: (a) [2-2FI] $(130-130)_{p-a}$ ($4 \times V_2$); (b) [2-2FI] $(130-156)_{p-a}$ ($4 \times V_2$).

Figure 8 is the replot against T_2 from Figure 7 of the Γ at 5 and 7 min, which corresponds to the state of preheating before the restretching mentioned in the preceding section. A rapid drop of Γ is seen above 150°C , which is considered to be caused by the larger premelting and disorientation (Fig. 3, a_1-d_1).

The Γ value of the specimen restretched after 5 min of preheating at T_2 is shown in Figure 9 as function of the degree of restretching, v_2 . The retardation immediately after the restretching is lower at $T_2 = 156^\circ\text{C}$ than at $T_2 = 130^\circ\text{C}$, owing to the enhanced premelting and disorientation in the former case. However, interestingly, values of Γ at room temperature are nearly equal to each other, irrespective of the difference in types of orientation induced by the two restretching processes. The recovery in Γ is smaller in cooling from 130°C than from 156°C , as mentioned above.

In general, the change in Γ is in good agreement with the changes observed in the x-ray photographs in the preceding section.

DSC Observation

A piece of film was uniaxially stretched $4\times$ at $T_2 = 130^\circ, 140^\circ, \text{ or } 150^\circ\text{C}$, and DSC analysis was carried out on each specimen. As shown in Figure 10, the thermogram of the specimen stretched at 130°C has a small shoulder. However, as T_1 rises higher, it disappears and the thermogram sharpens. In all cases the melting range is $130\text{--}170^\circ\text{C}$.

In the following analysis, three points are defined and plotted against T_1 , as shown in Figure 11. T_m is the melting point which is read at peak temperature a (Fig. 10), and $T_{1/2}$ and $T_{2/3}$ are the temperatures at b and c (Fig. 10), where the melting enthalpy amounts to $1/2$ and $2/3$ of the total melting enthalpy ΔH , respectively. The hatched portion is the transition region from type II into type III orientation previously reported.¹

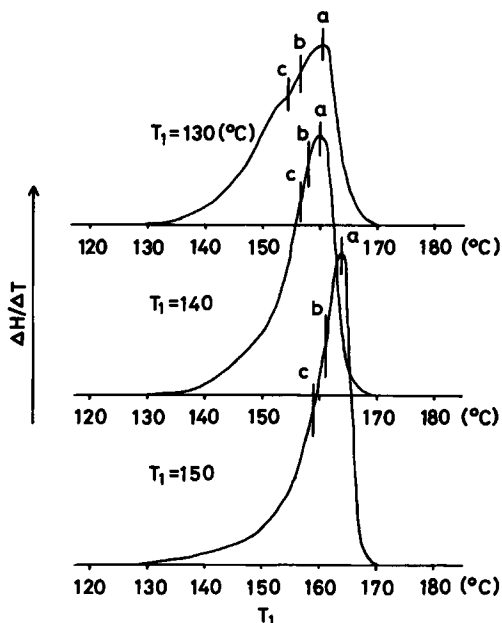


Fig. 10. DSC thermogram of film uniaxially stretched at various temperatures ($4\times$); (a) T_m ; (b) $T_{2/3}$; (c) $T_{1/2}$.

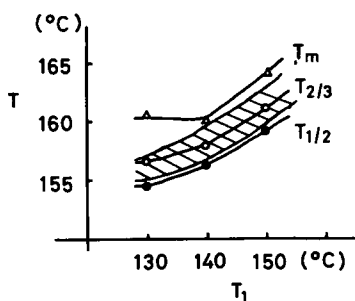


Fig. 11. Relations between T_1 and T_m , $T_{1/2}$, and $T_{2/3}$.

It is concluded from the figure that calorimetrically, a nearly equal fraction ($1/2-2/3$) of crystallites is melting for the appearance of type III orientation when the specimen undergoes the restretching at any T_2 , which is also a function of T_1 . Such a great extent of premelting is in good accordance with the x-ray observation mentioned above.

CONCLUSIONS

It is evident from the experimental results mentioned above that the extent of premelting at 130°C differs much from that above 150°C , and this difference is the cause of the two types of orientation. At 130°C , it is reasonable to consider that the crystalline lamellae are comparatively sound and that the lamellae rotate as a whole during restretching, as already described. However, above 155°C a considerable fraction premelts, and the mosaic structure of the lamella loosens so significantly and the crystalline lattice is distorted so much that the unfolding predominates rather than the rotation of the lamella as a whole. This is the cause of type III orientation.

In order to illustrate the deformation mechanism more clearly, Peterlin's model is useful.⁵ The fine structure of polypropylene film stretched $4\times$ at 130°C is considered to be as shown in Figure 12, namely, it consists of groups of parallel bundles of microfibrils (MF). When it is restretched, a stress is applied on these groups to rotate them.

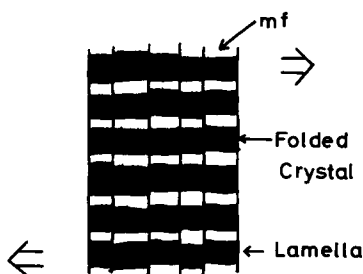


Fig. 12. Schematical illustration of fine structure of uniaxially stretched film.

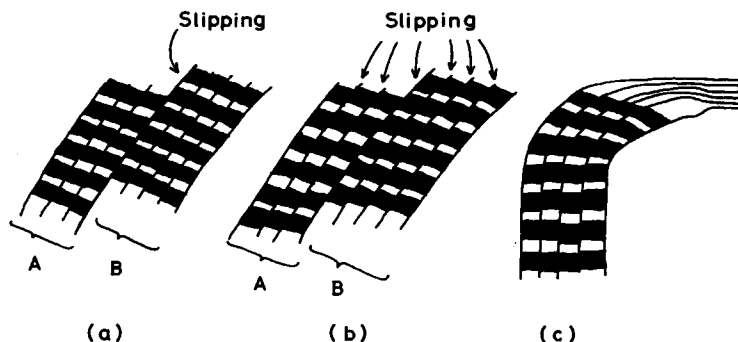


Fig. 13. Schematic illustration of deformation during restretching: (a) deformation at 130°C, yielding type II orientation; (b) deformation at 150°C, yielding type II orientation; (c) deformation at 156°C, yielding type III orientation.

The structure composed of these microfibrils is not uniform, but there are irregularities of various orders: (1) within the MF itself, (2) between MF's, and (3) between the groups of MF's. These irregularities as well as the increasing thermal distortion play a role in deformations of various types. These irregularities seem to be relevant to the irregularities of the original structure, such as mosaic structure of lamellar crystal and crystalline defects derived from macro- and microtacticity and the irregularities produced during stretching process.

When T_2 is 130°C, only the third irregularity is effective and rotation of the groups occur by slipping between them (A and B), as shown in Figure 13a. The lamella appears to rotate as a whole, and a simple relation holds between the observed long period L and the angle θ between the c -axis and the normal to the lamellar surface.¹ Here,

$$L = L_0 \cos \theta$$

where L_0 is the value of L before restretching. However, as T_2 rises further, the second irregularity is also effective and slippage now occurs within the rotation groups A and B, i.e., between MF (Fig. 13b), and the simple relation above mentioned fails to hold. In these two cases the orientation is of type II. The details will be described in the following paper.

When T_2 is elevated above 155°C, the first irregularity plays a principal role, and micronecking (unfolding) starts and develops further and further as the degree of restretching grows (Fig. 13c). Upon cooling, the unfolded chains crystallize into intermolecular crystals, aligning parallel to ps , and the lamellar crystals partly continue orienting more or less in the direction pp ; hence, type III orientation results. It is easily seen from the x-ray (Fig. 3), optical (Fig. 7), and DSC (Figs. 8 and 9) studies that the effectiveness of the first irregularity is the result of violent thermal motion of the chains within the crystalline phase.

At high temperatures, the restretching breaks up the lamellae into smaller-sized mosaic blocks corresponding to the diameter of MF and also

distorts the lattice; hence the x-ray pattern becomes a halo. However, during cooling after restretching, the segments which were premelted during the previous heating recrystallize on the remaining crystallites and nuclei, and the broken-up small crystals reorganize into lamellae. The pulled-out chains also crystallize in direction *ps*, the crystalline type of which may be predominantly intermolecular, because small-angle x-ray scattering pattern indicates no evidence of lamellar crystal stacking in the direction *ps*, as shown in Figure 4 of reference 1. Recrystallization into lamellar crystal is so scanty and/or so imperfect that it is not discernible in small-angle x-ray scattering if it exists at all in such high-temperature restretching.

Thus, the finished film attains type III orientation. However, disorientation after restretching proceeds speedily at such high temperatures, and clear type III orientation fails to appear unless the film is cooled immediately after restretching. As a result, it is summarized that the main

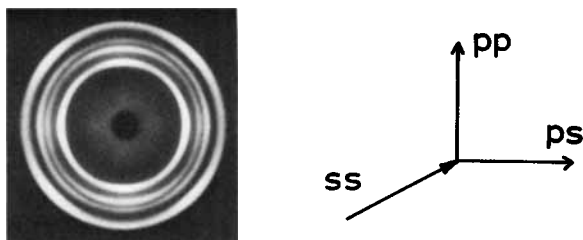


Fig. 14. Diffraction pattern of type III orientation: $[2-2FI](130-157)_p(4 \times 3)$.

factor yielding type III orientation is the relative easiness of unfolding compared with that of the lamellar rotation. This view is also supported by the phenomenon that type III orientation preferentially appears when the restretching is carried out when the film width is restrained, under which condition the rotation of lamellae should be severely restrained.

At present, the authors envision the restretching process in such a way. However, the mechanism proposed above as a possible explanation contains some speculations and problems to be solved by further study. For example, an interesting phenomenon is that the (040) intensity is considerably weaker in comparison with that of (130) on the equator, while it is reverse on the meridian, as shown by a typical example of type III orientation in Figure 14. This may be evidence that the crystallites newly developed in *ps* are of a different type from those remaining in *pp*, and this is important for describing the restretching process in detail.

The authors wish to thank Dr. Masahide Yazawa of the Polymer Processing Research Institute for financial support. They are also grateful to Nippon Kogaku K.K. for helping the measurement of retardation by the auto-ellipsometer used in this study.

References

1. S. Okajima, N. Iwato, and H. Tanaka, *J. Polym. Sci. B*, **9**, 797 (1971).
2. H. Tanaka, K. Kurihara, M. Morita, K. Mori, and S. Okajima, *J. Polym. Sci. B*, **9**, 723 (1971).
3. H. Tanaka T. Masuko, and S. Okajima, *J. Appl. Polym. Sci.* **17**, 1715 (1973).
4. H. Awaya, *Nippon Kagaku Zasshi*, **82**, 1575 (1961).
5. F. J. Baltá-Calleja and A. Peterlin, *J. Macromol. Sci.—Phys. B*, **4**(3), 519 (1970).

Received October 17, 1972

Revised December 29, 1972